Research Paper

Utilization of Neural Network in Seismic Refraction Data Processing

Reza Khajavi[1], Gholam Javan-Doloei[2*], and Naimeh Khorshidi[3]

1. Assistant Professor, Ferdowsi University of Mashhad, Mashad, Iran
2. Associate Professor, Seismology Research Center, International Institute of Earthquake Engineering and Seismology (IIEES), Tehran, Iran,
*Corresponding Author; email: javandoloei@iiees.ac.ir
3. M.Sc. Student, Ferdowsi University of Mashhad, Mashad, Iran

ABSTRACT

Increasing our understanding of the earth's layering characteristics at an engineering scale is crucial for the optimal design of tall buildings, important industrial facilities, and lifelines infrastructures. The most important characteristics that can be measured by the seismic refraction method are the speed of longitudinal and transverse seismic waves. In addition, determining the thickness of layers up to depth of 150 m is another capability of this method. In this research, the classical refraction seismic method has been compared with methods based on artificial intelligence techniques with emphasis on two types of fully connected and convolution techniques. The results of this research show that by replacing the neural network that fits the characteristics of the subsurface layers instead of using classical inversion methods, the accuracy of classical inversion methods can be achieved in much less time. Fully connected and convolutional neural networks are highly capable for identifying geological structures whose measurement data is contaminated with noise, with acceptable accuracy without pre-processing. Therefore, the proposed method, in addition to the ability to detect the arrival time of seismic phases in noisy signals and the time-consuming process of manual processing, is likely to be useful for identifying complex geological formations.

1. Introduction

Exploration geophysics is usually divided in two categories: seismic and non-seismic method. Seismic methods are classified into seismic reflection and seismic refraction subdivisions. In the seismic reflection method, the reflection of seismic waves from layers with a sudden change in speed is used. While in the refraction seismic method, the rays pass to the interface of two layers with a critical angle of incidence and travel a certain distance with the speed of the lower layer as a head wave (refraction wave) and then arrive to the receiver at the free surface. The use of reflection and refraction seismic methods for exploration purposes from sallow surface depth to a depth of about 50 km is common in the engineering scale, oil exploration and crustal structure studies. These processes can be carried out through three subdivisions [1]:

1) near surface studies (geotechnical explorations, underground layering and detection of underground cavities up to a depth of several meters, etc.);

2) medium depth exploration entitled hydrocarbon reservoirs studies; and

3) identification of deep layers of the crust.

Major seismic studies with the aim of preparing a subsurface image include the following steps [2-3]:

1) Design of seismic operations;
2) seismic data acquisition;
3) data processing to generate optimum velocity model and seismic section;
4) interpretation of results and seismic sections to identify different seismic.

Seismic exploration projects, in all four stages above, are very costly and time consuming. Therefore, any effort to reduce costs and increase economic efficiency in various stages of project will be very valuable and desirable. In particular, seismic and tomography inversion is a time-consuming procedure with a high processing cost in practical projects. Sometimes a large amount of processing is done sequentially to achieve convergence of results. These processing costs increase dramatically for new and updated methods. In addition to the challenges of seismic data processing, other complex difficulties such as noise effects, hidden layers and blind zones should not be overlooked.

This research deals with step (3) and processing stage that aims to make the optimum velocity structure model, easy, and economical. The science of Artificial Intelligence (AI), (machine intelligence), deals with the concept of intelligence in man-made machines and their ways of making them intelligent, and tries to recreate and customize an efficient balance of intelligence as a substitute for human natural intelligence. From this point of view, artificial intelligence refers to systems that can show reactions similar to intelligent human behavior, which is referred to as deep learning. In this new paradigm, instead of using the rules made by the human mind (which are represented in the form of a differential equation or an optimization problem in solving direct and inverse problems), an artificial brain is designed based on appropriate rules and observation. In the last five decades, the application of artificial intelligence has been assigned a special place in most branches of human sciences and techniques. The use of neural networks in exploratory methods is worthy of follow-up and investi- gation for the following reasons:

1. Geophysical exploration methods (in different stages, including inversion) are very time-consuming and have a high processing cost. It seems that artificial intelligence models, independently or in combination with classical inversion methods, provide the possibility of reducing processing costs. Also, empowering the classic methods of geophysical explorations with the help of artificial intelligence tools will be the basis for the use of complex methods in seismic surveys, which will greatly help to reduce the costs of such explorations.

2. There are various technical problems in seismic refraction and reflection methods (especially in identifying complex subsurface models, and anomalies, heterogeneities, and underground cavities). Identifying and categorizing these challenges on the one hand, and the possibility of reducing or eliminating them with the help of artificial intelligence tools, is a worthy effort

3. The ability of artificial intelligence and deep learning methods in near-surface inversion and refraction seismic methods has not been investigated deeply. From this point of view, it is necessary to investigate the effectiveness of this new paradigm in reducing processing costs and solving the technical challenges of identifying underground structures near the surface.

In this study, our goal is to identify suitable structures of artificial neural network and deep learning in inversion of data collected with refraction seismic method. The general results show the ability of proposed technique to reduce processing time and its cost. Obviously, this will be a way to solve the practical challenges of refraction seismology.

2. Literature review

In the recent years, artificial intelligence has been widely used and studied in reflection seismology and hydrocarbon reservoir exploration [4]. These studies are followed in the three areas; simulation of wave propagation and generation of synthetic seismic data, seismic imaging and inverse problems (velocity model building), and seismic interpretation (identification of seismic events, faults and geological structural features, etc.). Significant development in computation speed, along with the enhanced levels of accuracy and computational robustness, has opened a clear

perspective towards such studies in all the three fields.

The promising results obtained in seismic inversion are now extended to newer research areas such as three-dimensional data processing, enhanced feature-extraction procedures, combined FWI-based methods, etc. Application of deep learning (DL) algorithms in different perspectives of seismology, seismic imaging and exploration, geophysical inversions, etc. independently or in combination with classical methods, has proved to significantly reduce time and costs in the processing, as well as enhancing the quality of results. Also, classical geotechnical investigation methods, equipped with artificial intelligence tools, have enabled the application of simpler methods and calculations, which efficiently reduce the costs for geophysical surveys. In some studies, a variety of methods have been proposed to combine modeling approaches based on physical laws and machine learning techniques, such as using the physical loss function to make deep learning models compatible with physical limitations [5]. Artificial neural networks have been quite successful in recognizing and reconstructing structural under ground patterns. This allows them to be used to identify and classify subsurface images.

Convolutional Neural Networks (CNN) have provided rapid advances in the classification and recognition of objects in images [6]. By training the convolutional neural network with the help of three-dimensional seismic data, Wrona et al. [7] obtained a significant reduction in the interpretation time to detect faults and salt domes out of geological structures. Hateley et al. [8] has proposed a DL algorithm for detecting subsurface seismic lines.

Exclusive networks for some seismological tasks such as fault detection [9], earthquake detection [10], depth detection [11], and seismic phase arrival time [12] have been proposed. Also, with the help of deep learning, it is possible to achieve the highest signal-to-noise ratio (PSNR) in seismic data while maintaining very useful information in both qualitative and quantitative aspects, compared to other methods [13]. In seismic early warning systems (EEWs), DL techniques provide opportunities to extract and exploit the characteristics of the full waveform. A

new earthquake rapid warning has been able to be issued with confidence after 4 seconds from the arrival of the initial P wave [14].

As other applications to geophysical inversion techniques, CNNs have now been able to provide an extensible framework for identifying ground-water reservoirs using seismic data. Key parameters such as the aquifer volume, water level, etc. may now be estimated from seismic data, which were not previously possible with seismic tomography or reflection procedures [15].

In addition, real-time determination of the focal mechanism of the earthquake source has been done by introducing a new method of deep learning, namely the focal mechanism network (FMNet) [16]. This network has been trained with 787320 artificial data and has been able to successfully calculate and present the focal mechanism of four earthquakes with a magnitude of 5.4 Mw. After receiving the data in less than 200 milliseconds, the network reliably predicted the focal mechanism of the source with a single processor. In another study, a convolutional neural network was designed and proposed to identify and evaluate underwater barriers. Numerical solution of the sound wave equation has been used to generate a sufficient amount of well-qualified data to train the network. Finally, it is possible to detect the position and geometry of any unknown dispersant in just a few milliseconds [17].

The use of neural networks in seismic refraction surveying methods, however, has not yet found a special place. As one of the few examples, in a research by Engelsfeld et al. [18], using the seismic refraction method, the effect of the presence of a void in a 2D two-layer geological model was investigated. The first wave arrivals are obtained to determine the position and size of circular voids. The application of these relationships in a natural rock environment has been tested and while confirming the accuracy of the method, its efficiency for detecting non-circular cavities has also been shown. The effect of different cavities on the propagation of the Rayleigh waves and the longitudinal P waves has been investigated with the help of synthetic traces generated by finite element models for cavities in different dimensions and depths [19].

3. Research Methodology

The research methodology is described in following three consecutive sections. In the first subsection, the method of constructing training data is introduced. In the second subsection, network design and selected architectures will be discussed; in the final subsection, the training and testing process is introduced.

3.1. Training Data Construction

In order to train, test and validate a neural network, a large amount of data is required. Since this volume of data may not practically be available by field acquisition, numerical simulation might rather be employed for the purpose. In this research, propagation of rays from the source through the near-surface substrates and generation of synthetic traces is simulated by a simple ray-tracing procedure, as will be explained as follows: The arrival times of direct, refracted and reflected rays to any receiver at a certain distance from the source are calculated. The attenuated Ricker wavelets are then shifted according to the arrival times for any receiver to form its regarding main trace. An appropriate level of White noise is then added to the signal to construct the final trace.

For the present ray-tracing simulation, it is assumed that underground velocity increases with deeper layers. Waves are propagated from a source on the earth's surface to a distance of x where is recorded by a receiver (Figure 1a). Based on the distance between the first receiver and the source,

the first arrivals of seismic energy may be direct or refracted waves (Figure 1b). Traces may also contain reflective phases as well, which provide additional information from underground layers, e.g. the presence of a layer with a velocity lower than the upper layer, which, of course, may not be revealed by refractive waves.

Typically, the length of the seismic profile should be more than four times the desired depth on the engineering scale, the maximum length of the seismic profile is less than 150 m, and the distance between the seismic receivers is determined differently depending on the amount of energy released from the source. For near-surface exploration, a distance of 5 m between receivers is suitable to detect anomalies with dimensions up to 2.5 m.

In this research, ray tracing process is applied by coding a MATHEMATICA-12 package named as Simulation, for which the stratification geometry, velocity model, receivers (geophones) arrangement, and noise level are considered as inputs. The package generates the received trace $A(t)$ at any arbitrary location x, as the output, by the following relation:

$$A(x;t) = A\psi(t - t_0) + N(t) \tag{1}$$

where ψ is the Ricker wavelet to model the source, A denotes the attenuated wave amplitude at the receiver, and $N(t)$ is the noise function. t_0 is the arrival time of the wave to the receiver, which may represent any of the direct, refracted or reflected waves based on the stratified media. In the following, the calculation of these parameters in the
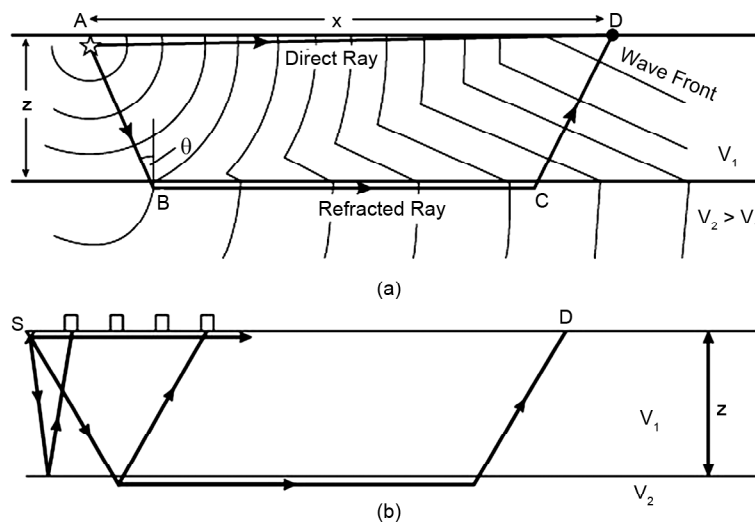

Figure 1. (a) Different rays in seismic refraction theory, (b) Different ray arrivals based on distance between receiver and source.

program is introduced.

3.1.1. Arrival Time

For a single horizontal layer of thickness z located on the infinite layer, the arrival time for the seismic wave to the receiver at a distance x from the source is obtained as:

$$t = \frac{x}{v_2} + \frac{2z\sqrt{v_2^2 - v_1^2}}{v_1 v_2} \qquad (2)$$

where v_1 and v_2 are the wave velocities for the first and second layers, respectively. Calculating the arrival times for reflective and direct waves is simple and is not reported here.

3.1.2. Amplitude

Seismic wave amplitude changes during propagation for various reasons. An important change is attenuation, due to two types of geometric and intrinsic damping mechanisms. In geometric attenuation, as the wave propagates, energy of the wavefront decreases as r^2 for spherical waves and as r^1 for surface waves, where r is the wave propagation distance. Thus, the amplitude A of the surface wave, dealt with in the seismic refraction method, decreases from amplitude A_0 at source as:

$$A = A_0 / r \qquad (3)$$

Attenuation of seismic waves due to inherent inelastic properties of the earth, such as mineral fractures, shear heating at the crystal boundaries, movements of liquids within cracks, or those created by refraction, reflection, and scattering, is called intrinsic attenuation. Inherent attenuation is simulated by the following relation:

$$e^{-\alpha x} A = A_0 \qquad (4)$$

where α is called the absorption coefficient or attenuation factor, which is the inverse of the quality factor and varies for different materials. Considering both geometric and intrinsic attenuations, the amplitude of the seismic wave, as it moves away from the source, is as follows:

$$A = \frac{A_0}{x} e^{-\alpha x} \qquad (5)$$

3.1.3. Noise

The accuracy of the geophone readings is strongly affected by the noise level. Noises in seismic data are generally divided into two categories. (1) Incoherent and random noise as a disturbance in amplitude which lacks any special order or coherence in the record. These random/white noises do not emanate from seismic energy sources; rather, they result from activities in the environment. This type of noise can be generated by trucks, vehicles, and people in the study area, as well as by near-surface scattering, wind, rain, power lines, and even animal traffic [20]. (2) Coherent noise that may add a redundant level of energy to the initial wave, so that a fixed phase from one trace to another is observed. Multiple reflections, surface waves such as ground rolls, air waves, coherent scattered waves, etc. are coherent noises that are usually present within seismic data. The source of seismic waves may cause some spatial cohesive noises as well. In this research, random white noise is only dealt with.

3.2. Network Architecture Design

After providing the training, testing and evaluation data, we may focus on network architecture design. In this research, a simple and a CNN network model are employed.

3.2.1. Simple Neural Network

As a first step, the simple model with a minimal architecture consisting of successive fully-connected layers is used, which focuses on global learning and ignores local patterns. Figure (2) illustrates a schematic view of the network with the dimensions of its middle layers. The output of the network is a three-component vector representing the depth of the first underground layer, as well as the velocities
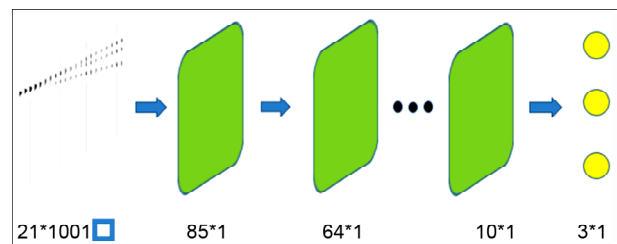
Figure 2. Neural network with seven fully-connected layers to fit the ground velocity model. The input is a matrix of 21×1001, and the output is a vector with 3 entries denoting v_1, v_2 and z. Dimension of hidden layer are selected by a trial-and-error procedure.

of the upper and lower ones. For training/test data simulation, a line of 21 receivers with 5 m distances is considered. Traces are simulated as Ricker wavelets of dilation 0.5, with different sampling rates as will be reported later, for a total period of 10 seconds; thus, inputs to the neural networks are $21 \times n_t$ matrices where the number of trace points n_t depends on the time resolution Δt.

3.2.2. Convolutional Neural Network

As a next step, the more sophisticated convolutional neural network CNN is used. Such networks are very efficient for detecting image patterns from pixel images with minimal preprocessing. CNNs identify pattern is in two steps. At the first step, the most important features are extracted (Feature Extraction) through convolution and pooling layers. Then, in the second step, a fully-connected layer performs the main task of identifying objects for classification.

In this research, a multi-layer CNN-based model is presented as a regression model for underground velocities out of linear-arranged traces introduced as an image. Figure (3) shows the proposed CNN, which consists of the following layers:
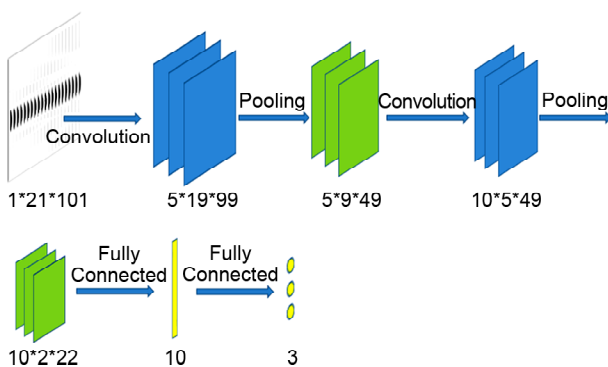
1. Convolution layer, in which correlation (rather than convolution) is performed by applying special filters. Such filters mark locales in the image with high similarity to special local patterns.
2. Relu rectifier, as a function that resets all negative pixels for a better highlighting of local patterns.

Figure 3. CNN to fit the ground velocity model. The input is a matrix of 21×1001, and the output is a vector with three entries denoting v_1, v_2 and z. Dimension of hidden layer are selected by a trial-and-error procedure.

3. Pooling layer, which is used to reduce the size of the input, increase the speed of calculations and more reliable detection of the features.
4. Fully-connected layer, to which all neurons of the previous layer are connected. The fully-connected layer combines the features to conclude the class which the input image belongs to.

CNNs need the inputs to be introduced as images; therefore, the input line of traces is converted to a gray-scale image with the dimensions of 101x21x1 for $\Delta t = 0.1$. The first layer (convolution) generates an output of a 99x5x19 array (also using the ramp activator function) through a correlation process and hands it over to the next pooling layer with a 2x2 filter and {2,2} stride, which produces an output of 49x9x5 array. The second convolution-pooling layers reduce the array to a 10x2x22 one, which is passed to the fully-connected layer where a 10 and a final 3-element vector is generated as a prediction for the velocity of the two underground layers and the thickness of the first layer.

3.2. Network Training Process

In this research, a total number of 50 images for input and 10 to 20 images for test data are produced. Standard deviations for velocities and depth are respectively considered as 50 and 0.1. It is notable that the training procedure is sensitive to depth variations. After preparing the training data and designing the appropriate network model, it is time to train the network, which requires specifying the loss function and the optimization algorithm. In this study, ADAM optimizer was used to update the weights. The method is popular due to its advantages over the standard Stochastic Gradient Descent algorithm. In this method, different learning rates are used for different parameters. These rates are adjusted based on the average recent values of the weight gradients. The algorithm works well for online and non-stationary problems. It should be mentioned that the design, training and testing of neural networks in this research are performed through programming in the MATHEMATICA software.

4. Results and Discussion

In this part, some examples of subsurface

structure are investigated with the proposed neural network method as well as the seismic refraction method. In all these samples, in order to construct the training data, a set of pre-assumed velocity models as well as their corresponding outputs (traces) for a two-layer underground model was provided with the help of the package Simulation written in MATHEMATICA. Figure (4) shows an example of a synthetic generated trace using simple ray tracing relations.
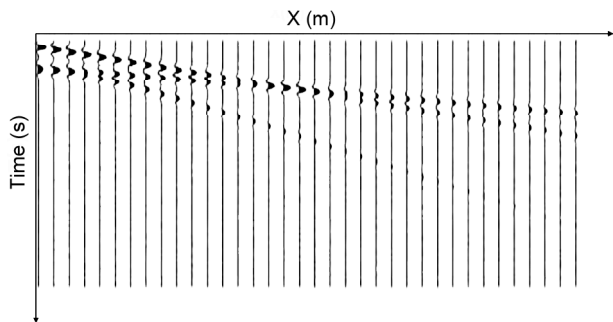

Figure 4. Synthetic seismic traces simulated for a two-layer underground model. Attenuated direct, refracted and reflected signals appear in the traces.

The length of the seismic profile is 100 m for this simulation, which is common in shallow seismic refraction operations, and the distance between the synthetic receivers is considered as 5 m to enhance spatial resolution. The seismic source is also set at a 5 m distance from the first receiver. The model is defined as a horizontal two-layer structure with a velocity of 250-350 m/s and a thickness of 8.5-7.5 m for the first layer and a velocity of 700-800 m/s for the second semi-infinite lower layer. 70% of the generated synthetic data (70 images) is considered for training and the remained 20% for test. Both simple network and CNN models are trained for the two noise-free and 5%-noise (on amplitude) cases with three- and one-variable outputs as shown in Figures (5) and (6). As can be seen, for both cases, overfitting is observed when noises are present.

Now, to examine and compare different methods and cases, the sample shown in Figure (7) is examined. The velocity of the first layer is 300 m/s with a thickness of 8 m and the velocity of the second layer is 750 m/s in half space. The resulting noise-free and noisy traces are shown in Figures (8a) and (8b), respectively.
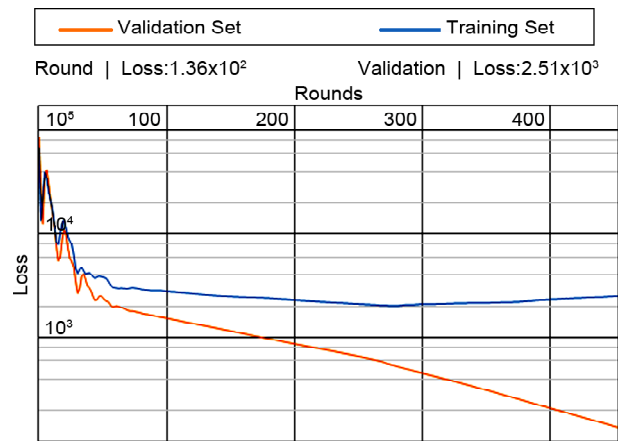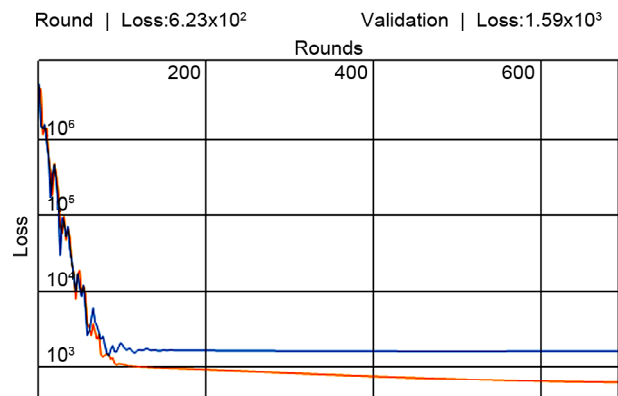

(a) Convolutional Neural Network with 5% Noise
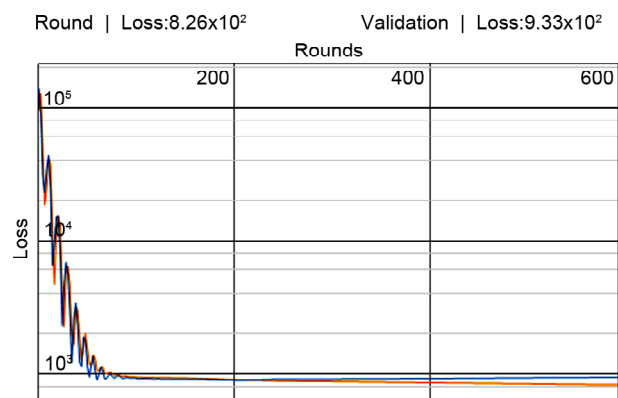
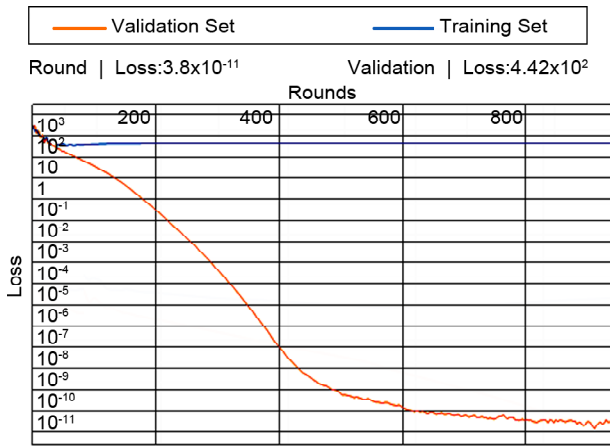(b) Convolutional Neural Network without Noise
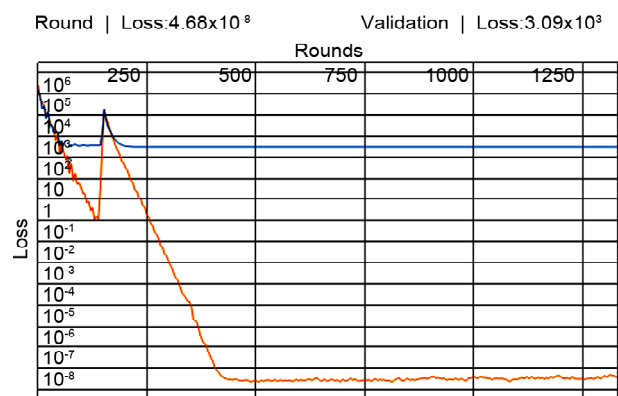
(c) Naïve Fully Connected Neural Network with 5% Noise
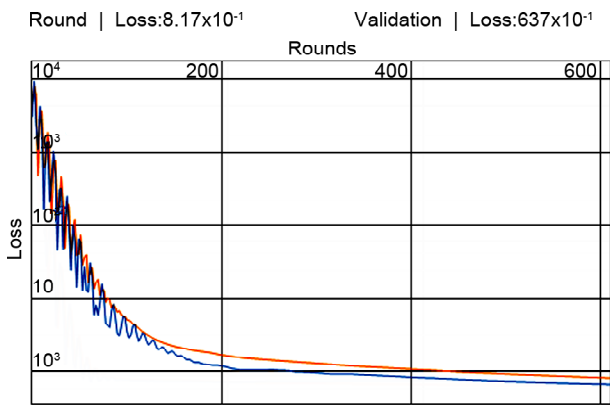

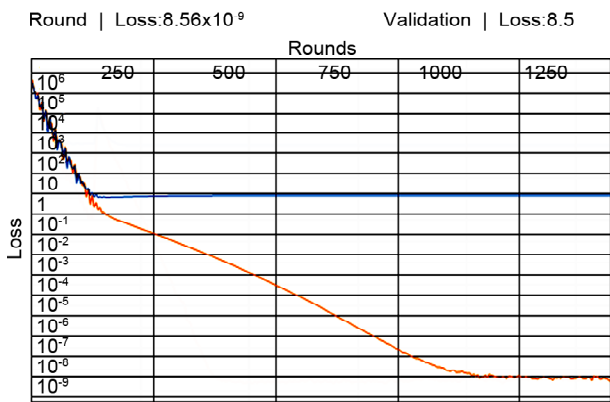(d) Naïve Fully Connected Neural Network without 5% Noise

Figure 5. Convergence diagram for neural network with three-way output. Orange and Blue curves denote learning convergence for train and test data, respectively.
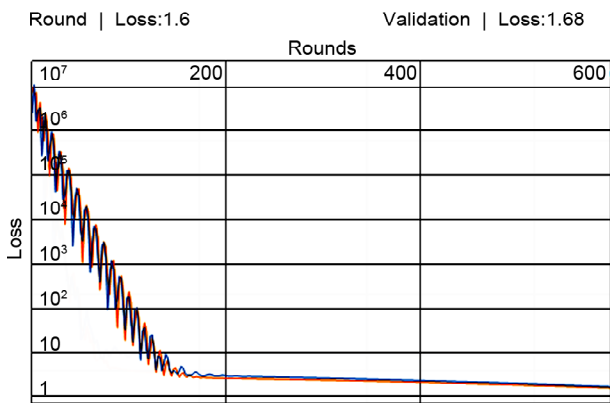
(a) Convolutional Network with 5% Noise

(b) CNN Free-Noise

(c) Naïve Fully Connected Neural Network with Noise 5%

(d) Naïve Fully Connected Free-Noise

Figure 6. Convergence diagram for neural network with univariate output h.
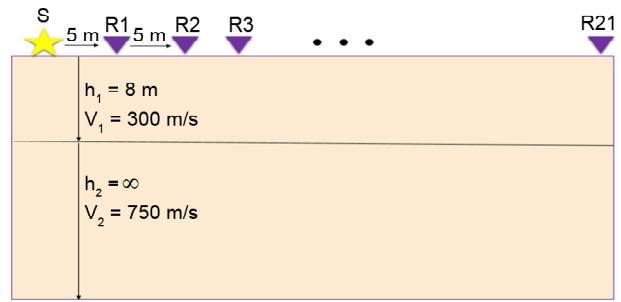
Figure 7. Horizontal two-layer underground model with the locations of source and receivers.

(a) Free Noise

(b) 5% Random Noise Cases
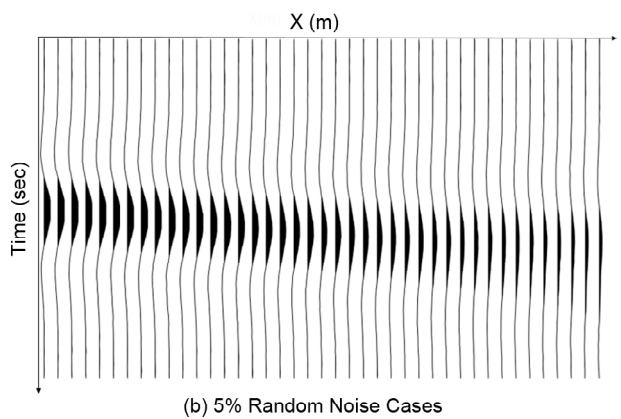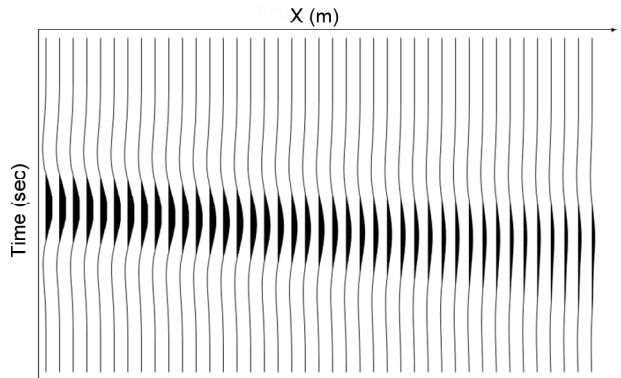
Figure 8. Synthetic traces for the horizontal two-layer model (The first 21 traces are used as input).

Three-component and single-component output results for the Simple Fully-Connected Neural Network (FCNN) and the CNN (with 50 training data and 12 test data) for both noise-free and 5% random noise cases are given in Tables (1) and (2), respectively. The results are compared with those obtained from the classical refraction method. According to the Tables (1) and (2), the lowest error is related to the fully connected neural network for the noise-free case, followed closely by the classical method, and the highest error pertains to the noise-free classical inversion. By comparing these two tables, it can be said that better results

are obtained for single-component output neural network. An important point is the low resolution 0.1 of the training data, which, by using NN technology has given appropriate results. Classical refraction methods, however, require resolutions around 0.001-0.00001 for acceptable results.

To further investigate the effect of sampling rate on the accuracy of artificial neural networks, these calculations were applied to the same designed neural networks with a sampling rate of 0.001. The results are reported in Tables (3) and (4) for three- and single-component outputs, respecti-

Table 1. Results for the two types of neural networks and the classical inversion method for the three-variable output mode.

Output	Actual Values	Inversion Classic		FCNN		CNN	
		Noise Free	Random Noise 5%	Noise Free	Random Noise 5%	Noise Free	Random Noise 5%
V_1 (m/s)	300	250	500	305.7	306.2	299.9	415.2
V_2 (m/s)	750	618.2	1307	750.1	708.3	743.8	785.2
H (m)	8	4.12	24	7.9	6.7	9.28	17.1
Absolut Error V_1 (m/s)	-	50	200	5.7	2.6	0.1	315.2
Absolut Error V_2 (m/s)	-	131.8	557	0.1	41.6	6.2	35.2
Absolut Error h (m)	-	3.88	16	0.1	1.3	1.28	9.1

Table 2. Results the two types of neural networks and the classical inversion method for the single-variable output mode.

Output	Actual Values	Inversion Classic		FCNN		CNN	
		Noise Free	Random Noise 5%	Noise Free	Random Noise 5%	Noise Free	Random Noise 5%
V_1 (m/s)	300	250	500	304.2	312.4	297.1	260
V_2 (m/s)	750	618.2	1307	753.9	789.4	750.8	718.6
H (m)	8	4.12	24	12.8	34.4	11.3	-4.6
Absolut Error V_1 (m/s)	-	50	200	4.2	12.4	2.9	40
Absolut Error V_2 (m/s)	-	131.8	557	3.9	29.4	0.8	31.4
Absolut Error h (m)	-	3.88	16	4.8	26.4	4.6	12.6

Table 3. Results for the two types of neural networks and the classical inversion method for the three-variable output mode.

Output	Actual Values	Inversion Classic		FCNN		CNN	
		Noise Free	Random Noise 5%	Noise Free	Random Noise 5%	Noise Free	Random Noise 5%
V_1 (m/s)	300	305.9	470	20700	4866	297.9	305.9
V_2 (m/s)	750	751.9	1424	-56283	-584	758	735.5
H (m)	8	8.2	17	41282	4081	7.6	11.1
Absolut Error V_1 (m/s)	-	5.9	170	920400	4566	2.1	5.9
Absolut Error V_2 (m/s)	-	1.9	674	57033	1298	8	14.5
Absolut Error h (m)	-	0.2	9	41274	4073	0.4	3.1

Table 4. Results for the two types of neural networks and the classical inversion method for the univariate output mode.

Output	Actual Values	Inversion Classic		FCNN		CNN	
		Noise Free	Random Noise 5%	Noise Free	Random Noise 5%	Noise Free	Random Noise 5%
V_1 (m/s)	300	305.9	470	20700	4866	297.9	305.9
V_2 (m/s)	750	751.9	1424	-56283	-584	758	735.5
H (m)	8	8.2	17	41282	4081	7.6	11.1
Absolut Error V_1 (m/s)	-	5.9	170	920400	4566	2.1	5.9
Absolut Error V_2 (m/s)	-	1.9	674	57033	1298	8	14.5
Absolut Error h (m)	-	0.2	9	41274	4073	0.4	3.1

vely. It should be pointed out that with the increase in the number of points for this case, the time for data generation and network training is doubled compared with the previous case.

The results show an increase in the accuracy of CNN outputs for both noise-free and noisy cases for the three-variable output case. For CNN single-component noisy case, the predictions are greatly modified. While the neural network is trained with velocity values of 250-350 m/s for the first layer, the prediction for a noise-free case with a velocity of the first layer equal to 500 m/s is 489 m/s, which implies good accuracy for the network. The overfitting error for the network is also removed.

To investigate the simultaneous effect of noise and sampling rate on the output accuracy of artificial neural networks, the three-variable CNN is trained by 50 noise-free data with sampling rates of 0.001 and 0.0001.

Again, the inputs are fed to the CNN trained with noise-free data and the sampling rate 0.001. For this case, the outputs are reported in Table (5). It is observed that even for high levels of noise, accuracy for velocity values are acceptable. For CNN trained with 50 noise-free data and a sampling rate of 0.0001, the outputs for different levels of noise are reported in Table (6). Compared with trained NN with data sampled at 0.001, higher accuracy is obtained. The accuracy of naïve fully-connected NNs with generated data sampled at 0.001 deteriorates, due to their higher error values during training data.

Table 5. Output of trained three-variable CNN with noise-free data and sampling rate of 0.001 at different noise levels.

Output	Actual Values	SNR				
		0	5%	10%	15%	30%
V_1 (m/s)	300	293	292.5	293.9	261.2	231.7
V_2 (m/s)	750	751	747.3	747.4	747.6	677.6
H (m)	8	12.6	13.8	14.5	19.9	64

Table 6. Outputs of trained three-variable CNN with noise-free data and sampling rate of 0.0001 at different noise levels..

Output	Actual Values	SNR				
		0	5%	10%	15%	30%
V_1 (m/s)	300	324.7	324.3	322.7	317.6	352
V_2 (m/s)	750	750.1	750.1	749.5	752.7	743
H (m)	8	12.1	12.7	10.6	16.5	0.29

5. Conclusions

In this research, we achieved an accuracy equal to classical inversion in a very short time during data processing based on artificial intelligence. Other results obtained in this research were the leaving aside the eye errors, peaking the first arrival of the wave, good accuracy in high sampling rate data processing using the convolutional neural network and very good accuracy for low resolution data using fully connected networks. Therefore, convolutional neural networks are more efficient in processing data with high sampling rate, especially contaminated with noise. Therefore generally, in order to overcome the upcoming challenges in collecting seismic data with high sampling rate with the aim of identifying geological structures with small dimensions, it is inevitable to use fully connected neural networks and convolutional neural networks. Reduction of calculation time and accuracy of results are among the advantages of these two neural networks in seismic studies. However, the use of artificial intelligence tools in inversion and subsurface findings is facing challenges that require more analysis and research. It is obvious that generating synthetic data based on simulation with finite difference and/or finite element methods requires time, cost and high processing volume. The use of alternative methods such as approximate modeling methods or the reusing of artificial intelligence in solving direct problems are solutions that require further investigation in the future.

References

1. Robinson, E.S. and Coruh, C. (1988) *Basic Exploration Geophysics.* John Wiley and Sons Ltd. International Ed edition, 562p.

2. Evans, B.J. (1997) *A Handbook for Seismic Data Acquisition in Exploration.* Society of Exploration Geophysicists, 320p.

3. Dondurur, D. (2018) *Acquisition and Processing of Marine Seismic Data.* Elsevier Publisher, 606p.

4. Nasrollah-Nejad, A., Allamehzadeh, M., and Javan Doloei, G. (2016) Estimating values of the maximum peak ground acceleration of a strong

motion by three models of artificial neural networks. *Bulletin of Earthquake Science and Engineering*, **3**(4), 1-19.

5. Willard, J.D., Jia, X., Xu, S., Steinbach, M.S., and Kumar, V. (2020) *Integrating Physics-Based Modeling with Machine Learning: A Survey.* ArXiv, abs/2003.04919.

6. Le Cun, Y., Bengio, Y., and Hinton, G. (2015) Deep learning. *Nature*, **521**, 436-444.

7. Wrona, T., Pan, I., Gawthorpe, R., and Fossen, H. (2018) Seismic facies analysis using machine learning. *Geophysics*, **83**(5), 1-34.

8. Hateley, J.C., Roberts, J., Mylonakis, K., and Yang, X. (2019) Deep learning seismic sub-structure detection using the frozen. *Journal of Computational Physics*, **409**, 109313.

9. Araya-Polo, M., Dahlke, T., Frogner, C., Zhang, C., Poggio, T., and Hohl., D. (2017) Automated fault detection without seismic processing. *The Leading Edge*, **3**(36), 208-214.

10. Perol, T., Gharbi, M., and Denolle, M. (2017) Convolutional neural network for earthquake detection and location. *Science Advances*, **4**(2), e1700578.

11. Wu, Y., Lin, Y., Zhou, Z., Bolton, D.C., Liu, J., and Johnson, P. (2019) Deep detect: A cascaded region-based densely connected network for seismic event detection. IEEE *Transactions on Geoscience and Remote Sensing*, **57**(1), 62-75.

12. Zhu, W. and Beroza, G.C. (2018) Phase net: A deep-neural-network-based seismic arrival time picking method. *Geophysical Journal International*, **216**, 261-273.

13. Sang, Y., Sun, J., Gao, D., and Wu, H. (2021) Noise attenuation of seismic data via deep multiscale fusion network. *Wireless Communications and Mobile Computing*, 1-8.

14. Zhang, X., Zhang, M., and Tian, X. (2021) Real-time earthquake early warning with deep learning. *Geophysical Research Letters*, **48**(5), 2020GL089394.

15. Lahivaara, T., Malehmir, A., Pasanen, A., Karkkainen, L., Huttunen, J.M.J., and Hesthaven, J.S. (2019) Estimation of groundwater storage from seismic data using deep learning. *Geophysical Prospecting*, **67**(8), 2115-2126.

16. Kuang, W., Yuan, C., and Zhang, J. (2021) Real-time determination of earthquake focal mechanism via deep learning. *Nature Communications*, **12**, 1432.

17. Kahana, A., Turkel, E., Dekel, S., and Givoli, D. (2020) Obstacle segmentation based on the wave equation and deep learning. *Journal of Computational Physics*, **413**, 109458.

18. Engelsfeld, T., Sumanovac, F., and Pavin, N. (2008) Investigation of underground cavities in a two-layer model using the refraction seismic method. *Near Surface Geophysics*, **6**, 221-231.

19. Rahnema, H., Mirassi, S., and Dal Moro, G. (2021) Cavity effect on Rayleigh wave dispersion and P-wave refraction. *Earthquake Engineering and Engineering Vibration*, **20**, 79-88.

20. Tiwari, R.K. and Rekapalli, R. (2020) *Modern Singular Spectral-Based Denoising and Filtering Techniques for 2D and 3D Reflection Seismic Data*. Capital Publishing Company, New Delhi, India.